

Microstructure and tensile properties of Mg–Li–Al–Zn based alloys with Ce addition

WU Li-bin, LIU Xu-he, WU Rui-zhi, CUI Chong-liang, ZHANG Jing-huai, ZHANG Mi-lin

Key Laboratory of Superlight Materials & Surface Technology of Ministry of Education,
Harbin Engineering University, Harbin 150001, China

Received 23 March 2011; accepted 27 April 2011

Abstract: Mg–5Li–3Al–2Zn– x Ce ($x=0$ –2.5; mass fraction, %) alloys were prepared by casting, and heat treatments of homogenization at 300 °C and solid solution at 370 °C were carried out. The microstructure and tensile properties of as-cast alloys and their evolutions after solid solution were investigated. The results show that with the increase of Ce content, Al₂Ce/Al₃Ce precipitates are formed and the alloys mainly consist of α -Mg, Al₂Ce, Al₃Ce and AlLi phases, and the amount of AlLi and Al–Ce intermetallics decreases after solid solution. The content and morphology of the second phases have important effects on the mechanical properties of the alloys; the alloy with 1.0%Ce content exhibits excellent tensile strength. The tensile strength and elongation of Mg–5Li–3Al–2Zn–0.5Ce alloy is remarkably improved by the solution strengthening effect because of the addition of Ce.

Key words: Mg–Li alloy; Ce; heat treatments; solution strengthening; tensile properties

1 Introduction

Due to the increasing demand for lighter components, Mg–Li alloys with optimum combination of low density and noteworthy ductility have interested many engineers and scientists for over half a century [1]. As the lightest structural materials with useful strength, Mg–Li system assumes potential applications in aerospace and automobile fields [2,3]. Mg is a HCP metal with a density of 1.74 g/cm³ and has poor formability. The addition of Li to Mg alloys lowers the density from 1.74 g/cm³ to 1.3–1.6 g/cm³, and results in the HCP structure of the matrix being replaced by the BCC structure, improving low temperature formability of Mg alloys [4,5]. However, Mg–Li alloys exhibit limitations of relatively low tensile properties, which inhibits wider use of the alloys [6].

Mg–Li alloys with Li content lower than 5.7% form a single α phase. β phase will be formed if the Li content is above 5.7% [7]. The focus of the present investigation is only on the alloys possessing α phase with the addition

of 5% Li. In the recent years, how to improve the mechanical properties of Mg alloys has been the main objective of many studies. The strengthening methods, such as grain refinement and formation of fine secondary phase particles, have been applied to improving the mechanical properties of Mg–Li alloys through adding various the third elements. At present, several ternary Mg–Li–X (where X=Al, Zn, Zr, Ag, Th, Si) alloys have been developed [1,8]. As the third elements, X and Zn have excellent potentials to further strengthen Mg–Li alloys because of the formation of intermetallic particles and suitable solid solubility in α phase [9–11]. From the results of the previous studies [12–14], RE elements, with certain special characteristics, are well known for their positive effects in Mg alloys.

Based on the background mentioned above, the based alloy in this study is designed as LAZ532 which has a nominal composition of Mg–5Li–3Al–2Zn, and an interesting combination of preferable strength and moderate ductility. As the effects of La-rich RE and mischmetal additions in the LAZ532 alloy have been analyzed [2,12], this work is to study the effects of Ce

Foundation item: Project (51001034) supported by the National Natural Science Foundation of China; Projects (2008AA4CH044, 2009AA1AG065, 2010AA4BE031) supported by the Key Project of Science and Technology of Harbin City, China; Project (HEUCF201210004) supported by the Fundamental Research Funds for the Central Universities, China; Project (20092304120020) supported by the Research Fund for the Doctoral Program of Higher Education, China; Project (11553054) supported by the Project of Science and Technology of Heilongjiang Province Education Department, China

Corresponding author: WU Rui-zhi; Tel: +86-451-82533026; E-mail: Ruizhiwu2006@yahoo.com
DOI: 10.1016/S1003-6326(11)61245-4

addition (ranging from 0 to 2.5%) and heat treatment on the microstructure and tensile properties of the alloy.

2 Experimental

The as-cast alloys were prepared from commercial purity Mg, Li, Al, Zn and Mg–18.67%Ce master alloy, in a vacuum induction melting furnace under the protective argon atmosphere. After heating at about 730 °C for 40 min, the melt was finally cast into a steel mold. The chemical compositions of the ingots were analyzed by inductively coupled plasma atomic emission spectroscopy (ICP-AES) and the results are listed in Table 1.

Table 1 Chemical composition of as-cast alloys (mass fraction, %)

Alloy	Mass fraction/%				
	Li	Al	Zn	Ce	Mg
Mg–5Li–3Al–2Zn	5.16	3.22	2.24	–	Bal.
Mg–5Li–3Al–2Zn–0.5Ce	5.00	3.01	2.26	0.56	Bal.
Mg–5Li–3Al–2Zn–1.0Ce	5.00	3.00	2.14	0.90	Bal.
Mg–5Li–3Al–2Zn–1.5Ce	4.61	3.26	2.02	1.41	Bal.
Mg–5Li–3Al–2Zn–2.0Ce	5.02	3.61	2.23	1.89	Bal.
Mg–5Li–3Al–2Zn–2.5Ce	4.78	3.40	2.03	2.31	Bal.

The obtained alloys were homogenized at 300 °C for 24 h in a vacuum furnace. Some specimens were heat treated at 370 °C for 12 h and then quenched in water. After grinding and polishing, the samples for microscopy observation were etched for 3–10 s with a solution of 2% (volume fraction) nitric acid in alcohol. The microstructure of alloys was observed on an optical microscope (OM) and scanning electron microscope (SEM) equipped with an energy dispersive spectrometer (EDS). The phase structure was identified by X-ray diffraction using Cu K_α radiation operating at 40 kV and 40 mA. The uniaxial tensile tests were performed on a universal testing machine at room temperature with an initial strain rate of $1.33 \times 10^{-3} \text{ s}^{-1}$. The fracture surface of the alloys was also observed by SEM.

3 Results and discussion

3.1 Microstructures of alloy

The microstructures of the solid-solution treated alloys are shown in Fig. 1. All of the alloys with 5% Li present a single α -Mg phase structure. Abundant particles visible in Fig. 1(a) are situated inside grains and at grain boundaries. Some maculae, just like the ones marked by the frame, may be oxidation holes formed during heat treatment. With the addition of 0.5% Ce, the occurrence of a number of short rod-like precipitates in

the alloy is observed, which becomes more distinct in Fig. 1(c) for numerous scattered rod-like phase can be found in the matrix. With increasing the Ce content, the amount of precipitates increases as expected. Furthermore, in Fig. 1(f), there are some irregularly shaped massive particles. The grain size of the alloys presents no significant variation with different Ce additions.

Figure 2 shows the XRD patterns of the alloys homogenized at 300 °C for 24 h. The based alloy is composed of α -Mg matrix and AlLi phase. Additional peaks of Al₂Ce phase appear after adding 0.5% Ce, as shown in Fig. 2(b). With increasing Ce content further, other peaks of Al₃Ce phase can be found in the spectra. However, the AlLi peaks weaken gradually with Ce addition, which may be attributed to the formation of Al–Ce phase consuming some Al atoms.

The evolution of the phase compositions of the alloys after solution treatment was analyzed by XRD and the results are shown in Fig. 3. Compared with the homogenized alloys, α -Mg and Al₂Ce/Al₃Ce phases are identified in the solution treated alloys; the AlLi peaks which present in the homogenized alloys disappear after solution treatment. In more details, the peak intensity of Al–Ce phase in solution treated alloys decreases to some extent, and only some weak characteristic peaks can be detected. The XRD analysis reveals that the Al–Ce phases will be formed arising from Ce addition, which results in the decrease of the amount of the AlLi phase. The solution treatment leads to a decomposition of AlLi phase. A certain amount of Al–Ce phases also dissolve during the heating progress despite of the high thermal stability of them, forming a solid solution with α -Mg matrix. Figure 4 shows the EDS results of the two morphological compounds in LAZ532–1.5Ce alloy. The EDS analysis indicates that the polygonal compound and rod-like compounds are both enriched in Mg, Al, and Ce elements, the atomic ratios of Al and Ce in the two types of compounds are 2.5 and 3.85 respectively. The latter one contains more Mg and Al, which suggests that there are relatively low content of Al–Ce phase precipitated. The EDS results further verify that the addition of Ce to LAZ532 alloy causes the formation of Al–Ce phase. From XRD analysis, they can be identified as Al₂Ce on Al₃Ce.

According to the previous investigations on the effects of RE in Mg alloys, adding Ce to the studied LAZ532 alloy only causes the new Al–Ce phase forming, without forming other phases regarding to Mg–Ce and Mg–Al–Ce. The possibility of compound forming between two elements can be estimated by the electronegativity differences. The larger electronegativity differences between two elements responds to the easier formability of compound. The Al atoms preferentially

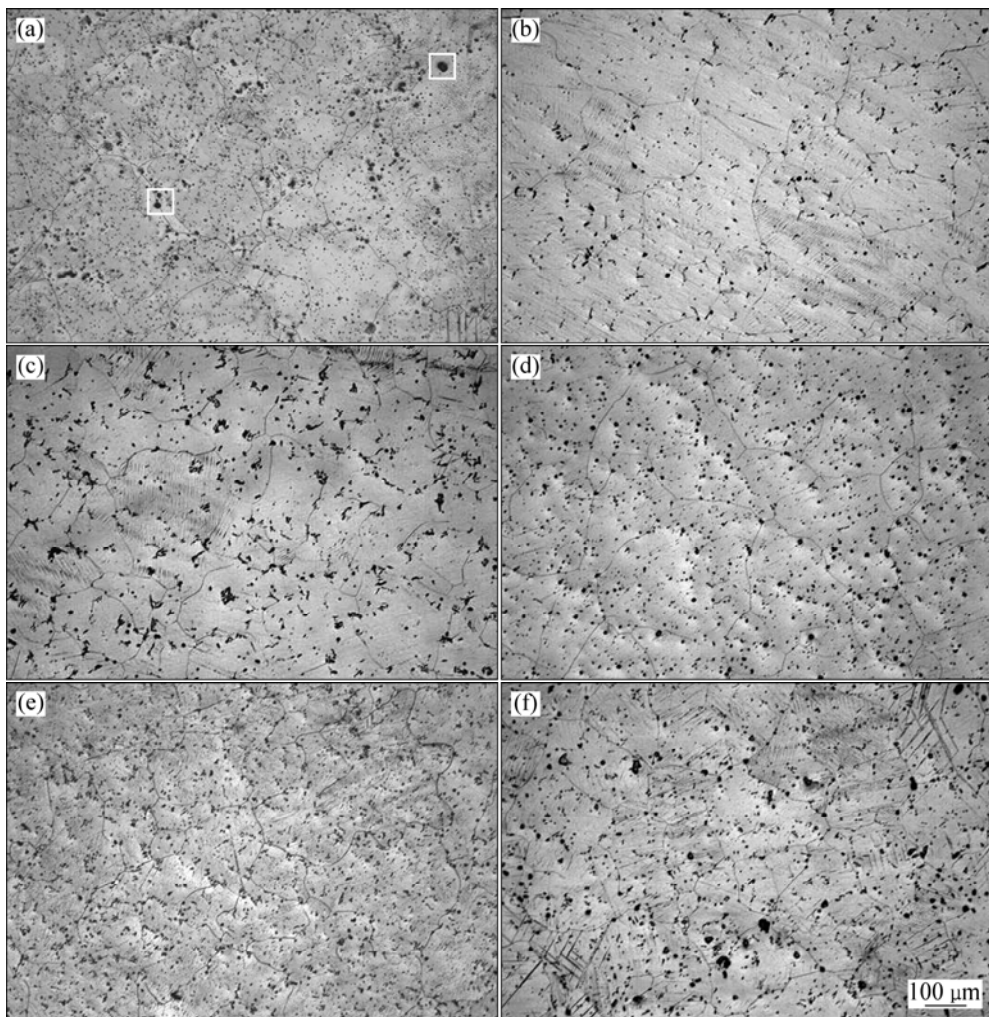


Fig. 1 Optical micrographs of solid-solution treated LAZ532-xCe alloys: (a) $x=0$; (b) $x=0.5$; (c) $x=1.0$; (d) $x=1.5$; (e) $x=2.0$; (f) $x=2.5$

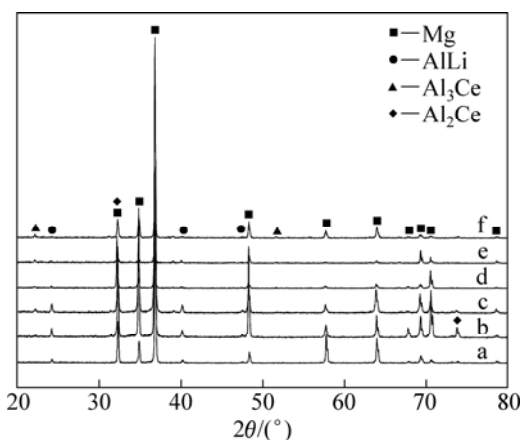


Fig. 2 XRD patterns of homogenized LAZ532-xCe alloys: (a) $x=0$; (b) $x=0.5$; (c) $x=1.0$; (d) $x=1.5$; (e) $x=2.0$; (f) $x=2.5$

interact with Ce atoms to form the $\text{Al}_2\text{Ce}/\text{Al}_3\text{Ce}$ because the electronegativity difference between them is relatively large [15]. During the solidification, the Ce elements commonly concentrate on the solid/liquid interface due to its equilibrium distribution coefficient

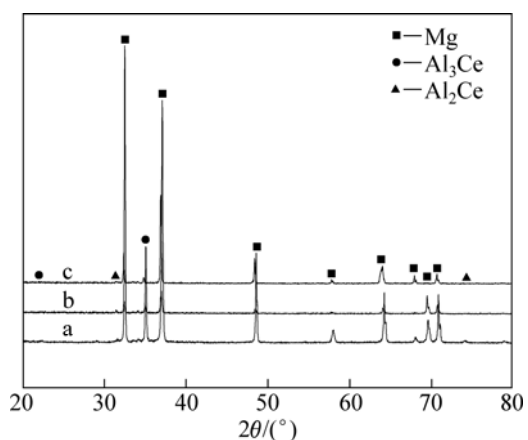


Fig. 3 XRD patterns of solid-solution treated LAZ532-xCe alloys: (a) $x=0.5$; (b) $x=1.5$; (c) $x=2.0$

$K<1$ and low solid solubility in α -Mg matrix, providing the obstacle for the diffusion of other elements. When the ratio of Al to Ce at the vicinity of the interface reaches the specific value, the Al–Ce phase is formed. In addition, the previous studies [16,17] reported that the

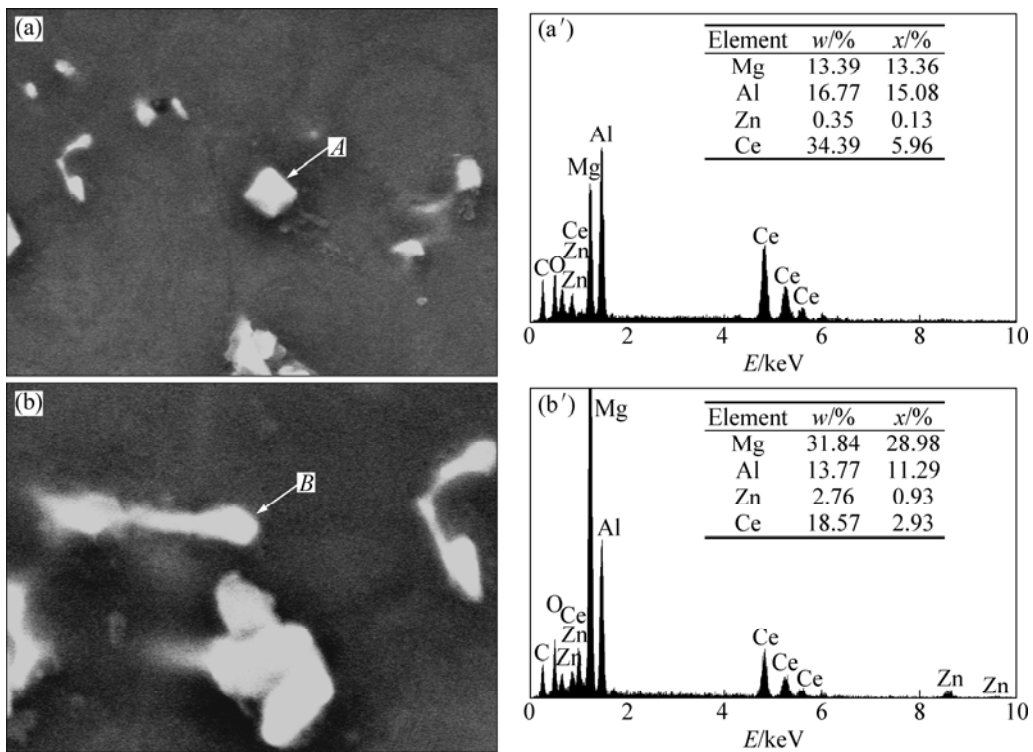


Fig. 4 EDS results of solution treated LAZ532-1.5Ce alloy: (a), (a') Polygonal compound; (b), (b') Rod-like compound

Nd addition influences the sorts of the Al–Nd phase. From the XRD results in the present study, when the Ce content is no less than 1%, the Al_3Ce peak is apparently observed in the spectra. Therefore, it can be drawn that increasing Ce addition promotes the Al_3Ce formation in this investigation.

The reasons for the unnoticeable grain refinement due to the Ce addition can be deduced as follows. Firstly, the constitutional supercooling arising from the concentration of elements on the solid/liquid interface improves the nucleation, and the particles generated around the grain boundaries can restrain the grain growth during solidification. These two factors are favorable for fine grains forming. Secondly, it is reported that the relative grain size (RGS) model proposed by EASTON and STJOHN [18] can predict the capacity on grain refinement coming from solute content:

$$d_{\text{RGS}} = 1 - \left(\frac{m_1 c_0}{m_1 c_0 - \Delta T_c} \right)^{1/P} \quad (1)$$

where d_{RGS} is the relative grain size; m_1 is the gradient of the liquidus slope; c_0 is the concentration of the solute; ΔT_c is the maximum constitutional under cooling and $\Delta T_c = m_1 c_0 (k-1)/k$; P is the supercooling parameter and $P=1-k$ (k is the partition coefficient for the solute). Al–Ce phase, which belongs to the cubic structure or hexagonal structure with lattice parameters greatly different from those of Mg, has no contribution to the heterogeneous nucleation. Conversely, it consumes a

large number of Al atoms and facilitates the RGS moving to the higher value, and XIAO et al [19] revealed that the Ce has a dramatic effect on grain size at low addition. However, it is possible that the AlLi phase formed in this study also plays an important role in grain refinement. For the 0.5%Ce alloy, the formation of AlLi phase is greatly restrained and the amount of precipitates is relatively low. As a result, the excellent refined structure is not obtained. From the analysis mentioned above, the interaction of positive and negative factors results in no noticeable difference in grain size after Ce addition.

3.2 Tensile properties

The tensile properties of the homogenized and solid solution treated alloys at room temperature are displayed in Figs. 5 and 6. Figure 5 reveals that, for the homogenized alloys, the tensile strength is essentially improved with increasing the Ce content up to 1%, where the alloy reaches the highest value of 218.54 MPa. After heat treatment, the tensile strength is initially enhanced but reduced when the Ce addition exceeds 1%. The 0.5%Ce-containing alloy obtains the optimal tensile strength of 233.05 MPa which is increased by almost 27% compared with that of the homogenized state alloy. Figure 6 shows that the similar trend is obtained on the elongation of the alloys. It is noted that the elongation exhibits a large elevation at relatively high Ce additions in homogenized state. This may be attributed to the excess of Al addition which is better for the elongation in

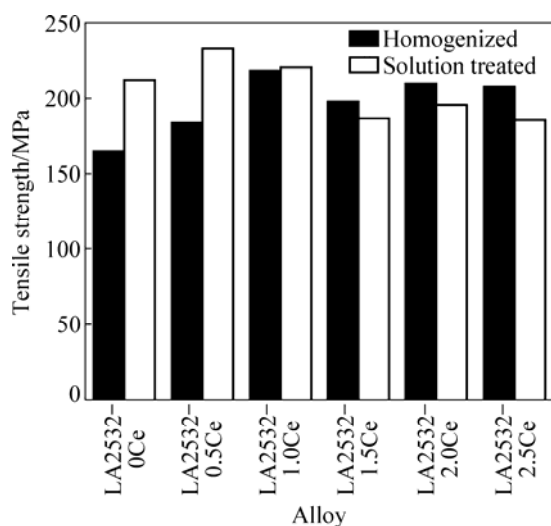


Fig. 5 Tensile strength of studied alloys

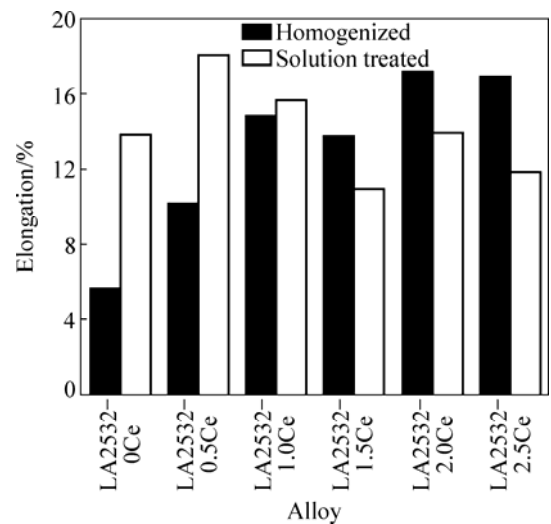


Fig. 6 Elongation of studied alloys

this study. After heat treatment, the alloy with 0.5% Ce has the best elongation of 18%.

It is known that Ce element has poor solid strengthening effect due to its limited solid solubility in α -Mg matrix [20]. In this study, it mainly precipitates as the form of $\text{Al}_2\text{Ce}/\text{Al}_3\text{Ce}$ compound during solidification. On one hand, these hard precipitates distributed in grains and at grain boundaries are expected to have a strong effect on strengthening the α -Mg matrix by hindering the movement of dislocations and the sliding of the grain boundaries, which contributes to enhancing the tensile strength. On the other hand, when adding high Ce content, the formation of Al–Ce phases consumes a large number of Al atoms and decreases the solute content in matrix, which leads to the reduction of solid strengthening effect. In addition, the Al–Ce phase also becomes relatively coarse with high Ce addition and, as a result, the strengthening effect provided by them is

compromised. These can be considered the main reasons accounting for the decrease of the tensile strength with high Ce additions. After heat treatment, the AlLi phase is almost dissolved due to the accelerated diffusion and the solid solution forms with α -Mg matrix. However, the Al–Ce phase with high thermal stability remains in the alloy. Thereby, the effects of solution strengthening and precipitate strengthening can be obtained simultaneously, thus the tensile strength of the 0.5%Ce-containing alloy with relatively high AlLi content is largely improved. The strengthening mechanism of the elongation improvement after heat treatment is similar to that of the tensile strength and is mainly due to the increased solute atoms in the matrix. The change in axial ratio c/a of the matrix, caused by solutes, such as Al, Li in this investigation, leading to a solid–solution softening on the nonbasal slip planes [21], contributes to a pronounced elongation.

3.3 Fracture analysis

The typical fracture surfaces of the alloys in both homogenized and solution treated states are shown in Fig. 7. Generally, the fracture of Mg alloys is brittle through the patterns of cleavage and quasi-cleavage because of the HCP structure of α -Mg [22]. From Fig. 7(a), it can be seen that the failure surface of the homogenized LAZ532–0.5Ce alloy consists of cleavage planes and steps, which belongs to the cleavage fracture. The similar fracture pattern is observed in the homogenized LAZ532–1.0Ce alloy. The difference is that there are more distinct ductile dimples on the surface of LAZ532–1.0Ce alloy. In Fig. 7(b) for the solution treated LAZ532–0.5Ce alloy, there are lots of ductile dimples attributed to the plastic fracture located on failure surface, corresponding to the great improvement of the elongation compared with the alloy in homogenized state. Moreover, the feature of cracked particles lying in the dimples indicates that cracks initiate on the second phase due to the stress concentration.

4 Conclusions

- 1) The homogenized LAZ532 alloy is composed of α -Mg and AlLi phases. With increasing Ce content, the rod-like and spherical $\text{Al}_2\text{Ce}/\text{Al}_3\text{Ce}$ phases are formed and distributed at grain boundaries or inside grains. After heat treatment, the AlLi phase is decomposed to α -Mg matrix while the $\text{Al}_2\text{Ce}/\text{Al}_3\text{Ce}$ phases almost remain in the alloy owing to their high thermal stability. Moreover, the grain refining effect of Ce additions is not obvious in this study.

- 2) The tensile strength and elongation of the alloy increase with the Ce content increasing, and the 1.0%Ce-containing alloy obtains the excellent values of

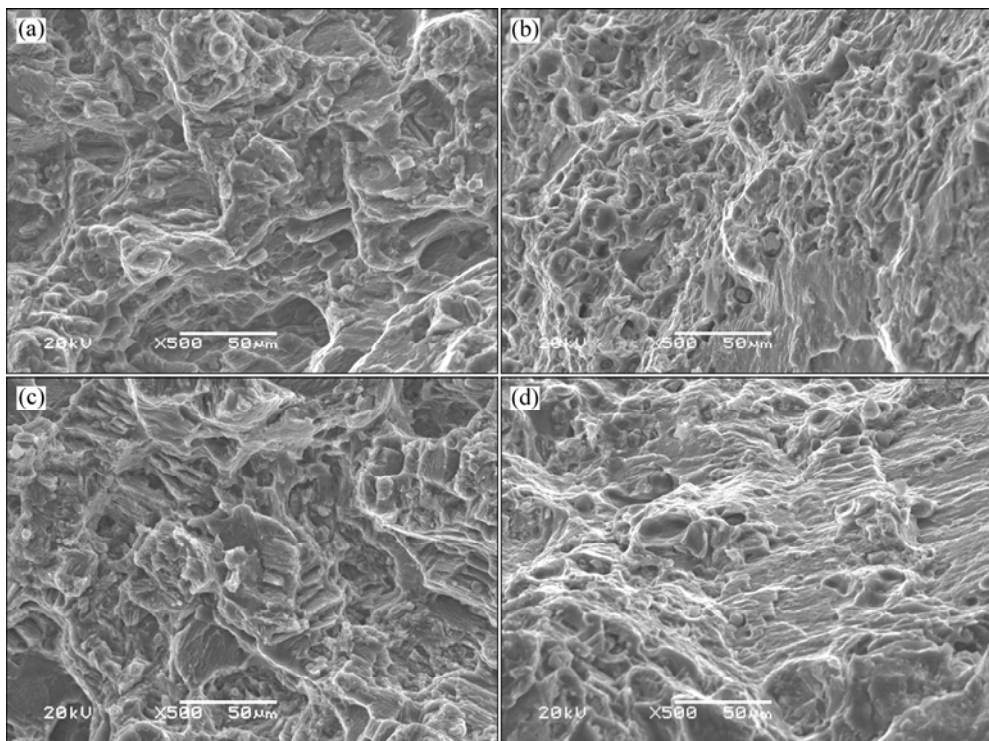


Fig. 7 SEM fractographs of LAZ532-xCe alloys before (a, c) and after (b, d) solution treatment: (a), (b) $x=0.5$; (c), (d) $x=1.0$

218.54 MPa and 15.36%, respectively. The solution treatment can further enhance the tensile properties, which is related to the solution strengthening effect. The best tensile properties are obtained for the solution treated LAZ532–0.5Ce alloy with tensile strength of 233.05 MPa and elongation of 18%, respectively.

3) Fracture analysis reveals that the homogenized LAZ532–0.5Ce alloy shows the cleavage fracture. The addition of 1.0% Ce causes pronounced plastic character as a number of dimples appear. Solution treatment makes the failure of the LAZ532–0.5Ce alloy tend to be mixed fracture.

References

- [1] RUSSELL A M, CHUMBLEY L S, GANTOVNIK V B, XU K, TIAN Y, LAAB F C. Anomalously high impact fracture toughness in B.C.C. Mg–Li between 4.2 K and 77 K [J]. *Scr Mater*, 1998, 39: 1663–1667.
- [2] WU L B, CUI C L, WU R Z, LI J Q, ZHAN H B, ZHANG M L. Effects of Ce-rich RE additions and heat treatment on the microstructure and tensile properties of Mg–Li–Al–Zn-based alloy [J]. *Mater Sci Eng A*, 2011, 528: 2174–279.
- [3] WANG Tao, ZHANG Mi-lin, WU Rui-zhi. Microstructure and mechanical properties of Mg–5.6Li–3.37Al–1.68Zn–1.14Ce alloy [J]. *Transactions of Nonferrous Metals Society of China*, 2007, 17: s444–s447.
- [4] SONG J M, WEN T X, WANG J Y. Vibration fracture properties of a lightweight Mg–Li–Zn alloy [J]. *Scr Mater*, 2007, 56: 529–532.
- [5] BUSK R S, LEMAN D L, CASEY J J. The properties of some magnesium-lithium alloys containing aluminum and zinc [J]. *Trans AIME*, 1950, 188: 949–951.
- [6] MATAUMOTO H, WATANABE S, HANADA S. Fabrication of pure Al/Mg–Li alloy clad plate and its mechanical properties [J]. *J Mater Process Technol*, 2005, 169: 9–15.
- [7] MENG X R, WU R Z, ZHANG M L, WU L B, CUI C L. Microstructures and properties of superlight Mg–Li–Al–Zn wrought alloys [J]. *J Alloy Compd*, 2009, 486: 722–725.
- [8] DROZD Z, TROJANOVA Z, KUDELA S. Deformation behaviour of Mg–Li–Al alloys [J]. *J Alloys Compd*, 2004, 378: 192–195.
- [9] KIM Y W, KIM DH, LEE H I, HONG C P. Widmanstaatten type solidification in squeeze casting of Mg–Li–Al alloys [J]. *Scr Mater*, 1998, 38: 923–929.
- [10] POLMEAR I J. Recent developments in light alloys [J]. *Mater Trans*, 1996, 37: 12–31.
- [11] WU Rui-zhi, ZHANG Mi-lin, WANG Tao. Microstructure characterization and mechanical properties of Mg–9Li–5Al–1Zn–0.6RE alloy [J]. *Transactions of Nonferrous Metals Society of China*, 2007, 17: s448–s451.
- [12] WU R Z, DENG Y S, ZHANG M L. Microstructure and mechanical properties of Mg–5Li–3Al–2Zn–xRE alloys [J]. *J Mater Sci*, 2009, 44: 4132–4139.
- [13] ZHANG M L, WU R Z, WANG T. Microstructure and mechanical properties of Mg–8Li–(0–3)Ce alloys [J]. *J Mater Sci*, 2009, 44: 1237–1240.
- [14] SU Gui-hua, ZHANG Liang, CHENG Li-ren, LIU Yong-bing, CAO Zhan-yi. Microstructure and mechanical properties of Mg–6Al–0.3Mn–xY alloys prepared by casting and hot rolling [J]. *Transactions of Nonferrous Metals Society of China*, 2010, 20: 383–389.
- [15] LIU H M, CHEN Y G, TANG Y B, HUANG D M, NIU G. The microstructure and mechanical properties of permanent-mould cast Mg–5wt%Sn–(0–2.6)wt%Di alloys [J]. *Mater Sci Eng A*, 2006, 437: 348–355.
- [16] ZHANG J H, WANG J, TANG D X, MENG J. Effect of Nd on the microstructure, mechanical properties and corrosion behavior of die-cast Mg–4Al-based alloy [J]. *J Alloys Compd*, 2008, 464:

556–564.

- [17] LIU B, ZHANG M L, WU R Z. Effects of Nd on microstructure and mechanical properties of as-cast LA141 alloys [J]. Mater Sci Eng A, 2008, 487: 347–351.
- [18] EASTON M A, STJHON D H. A model of grain refinement incorporating alloy constitution and potency of heterogeneous nucleant particles [J]. Acta Mater, 2001, 49: 1867–1878.
- [19] XIAO W L, SHEN Y S, WANG L D, WU Y M, CAO Z Y. The influences of rare earth content on the microstructure and mechanical properties of Mg–7Zn–5Al alloy [J]. Mater Des, 2010, 31: 3542–3549.
- [20] DAS S K, DAVIS L A. High performance aerospace alloys via rapid solidification processing [J]. Mater Sci Eng A, 1988, 98: 1–12.
- [21] LIM H K, KIM D H, LEE J Y, KIM W T, KIM D H. Effects of alloying elements on microstructures and mechanical properties of wrought Mg–MM–Sn alloy [J]. J Alloys Compd, 2009, 468: 308–314.
- [22] LV Y Z, WANG Q D, ZENG X Q, DING W J, ZHAI C Q, ZHU Y P. Effects of rare earths on the microstructure, properties and fracture behavior of Mg–Al alloys [J]. Mater Sci Eng A, 2000, 278: 66–76.

Ce 含量对 Mg–Li–Al–Zn 合金显微组织和拉伸性能的影响

吴利斌, 刘旭贺, 巫瑞智, 崔崇亮, 张景怀, 张密林

哈尔滨工程大学 超轻材料与表面技术教育部重点实验室, 哈尔滨 150001

摘要: 制备了 Mg–5Li–3Al–2Zn– x Ce($x=0$ –2.5; 质量分数, %)铸态合金, 并将所得合金分别于 300 °C 和 370 °C 进行均匀化和固溶处理; 研究固溶处理后合金显微组织和拉伸性能的变化。结果表明, 合金中加入 Ce 后出现 Al₂Ce/Al₃Ce 析出相, 此时合金主要由 α –Mg、Al₂Ce、Al₃Ce 和 AlLi 相组成; 固溶处理后合金中 AlLi 和 Al–Ce 析出相数量减少。析出相的数量与形态对合金的力学性能十分重要, 含有 1.0%Ce 的合金获得了优良的拉伸性能。固溶处理后 Mg–5Li–3Al–2Zn–0.5Ce 合金的强度和伸长率都得到了大幅度的提高, 这是因为合金在固溶处理后由于基体中的溶质原子增加而获得良好的固溶强化作用。

关键词: 镁锂合金; 钆; 热处理; 固溶强化; 拉伸性能

(Edited by YANG Hua)